Available online at www.sciencedirect.com

ScienceDirect

Advances in Space Research 57 (2016) 1345–1359

ADVANCES IN SPACE RESEARCH (a COSPAR publication)

www.elsevier.com/locate/asr

Ionospheric characteristics prior to the greatest earthquake in recorded history

C.U. Villalobos [a,1], M.A. Bravo [b,2], E.M. Ovalle [c,3], A.J. Foppiano [c,*]

[a] *Facultad de Educación, Universidad Adventista de Chile, Casilla 7-D, Chillán, Chile*

[b] *Instituto Nacional de Pesquisas Espaciais, Divisao de Aeronomia, Avenida dos Astronautas, 1758, Jardim da Granja, São José dos Campos, SP CEP 12227-010, Brazil*

[c] *Departamento de Geofísica, Universidad de Concepción, Casilla 160-C, Correo 3, Concepción, Chile*

Received 1 June 2015; received in revised form 30 July 2015; accepted 10 September 2015
Available online 25 September 2015

Abstract

Although several reports on the variations of some radio observed ionospheric properties prior to the very large Chile earthquakes of 21–22 May 1960 have been published, no one up to now has reported on the variations of simultaneous E- and F-region characteristics observed at Concepción (36.8°S; 73.0°W) using a ground based ionosonde. This paper analyses values of the NmE, NmEs, h'E, NmF2, h'F, M3000F2 and fmin. Possible solar and geomagnetic activity effects are first identified and then anomalies are calculated for all characteristics using reference values (15-day running medians ± interquartile range). Occasions when anomalies are larger than an upper threshold and less than a lower threshold are discussed and compared, whenever possible, with other published studies. Further study is suggested to unambiguously associate some found possible Es-layer and M3000F2 anomalies with very strong earthquakes.

Keywords: Ionospheric characteristics; Earthquake precursors; Chile

1. Introduction

For over the last half a century many attempts have been made to identify precursors of strong earthquakes (e.g. Biagi et al. (2012) – a special issue dedicated to this subject), even lately using satellite gravity field observations (Shahrisvand et al., 2014). In the case of ionospheric precursors, some sort of reference for a given ionospheric characteristic is first derived. This must take into account all possible solar and geomagnetic variability. Only then an anomaly can be accurately calculated for hours to days before the earthquake. These anomalies are to be analysed to search for an ionospheric precursor. For a consolidated review of this type of statistical analyses see Pulinets and Boyarchuk (2004). Later references are given by Ovalle et al. (2013) who discuss total electron concentration (TEC) and maximum electron concentration (NmF2) anomalies for the Chilean 27 February 2010 earthquake. Obviously, a key point in determining anomalies is whether it is possible to screen tropospheric/stratospheric variability that reaches the ionosphere (Forbes et al., 2000; Mendillo et al., 2002; Lăstovička, 2006) from the observed ionospheric variability so as to identify likely precursor ionospheric signatures.

A large variety of studies have been put forward suggesting likely mechanisms to justify the association between observed precursor ionospheric anomalies and seismic

* Corresponding author. Tel.: +56 41 2203083.
E-mail addresses: carlosvillalobos@unach.cl (C.U. Villalobos), manuel.bravo@dae.inpe.br (M.A. Bravo), eovalle@dgeo.udec.cl (E.M. Ovalle), foppiano@udec.cl (A.J. Foppiano).
[1] Tel.: +56 42 2433629.
[2] Tel.: +55 123 2087182.
[3] Tel.: +56 41 2203153.

http://dx.doi.org/10.1016/j.asr.2015.09.015
0273-1177/

activity occurring before strong earthquakes. Pulinets and Boyarchuk (2004) extensively review these proposed mechanisms. An up to date comprehensive report on how information could be conveyed from the Earth´s surface to the ionosphere through the Global Electric Circuit is given by Pulinets and Davidenko (2014).

On statistical studies, even the possibility to identify ionospheric precursors has been somewhat controversial as epitomized by Rishbeth (2007) and Pulinets (2007) a decade ago. Recently this controversy has again aroused some interest. Heki (2011) detected a clear precursory positive anomaly of TEC around focal region of the 2011 March 11 Tohoku-Oki earthquake using data from the Japanese dense network of Global Positioning System (GPS). The anomaly started ~40 min before the earthquake and reached nearly ten percent of the background TEC. He also suggested that similar anomalies were seen in the 27 February 2010 Chile earthquake, and possibly in the 2004 Sumatra-Andaman and the 1994 Hokkaido-Toho-Oki earthquakes, but not in smaller earthquakes. However, an alternative interpretation of the TEC variation in the ionosphere associated with the 11 March 2011 Tohoku-Oki earthquake is given by Kamogawa and Kakinami (2013) on the basis of the work of Kakinami et al. (2012). Their interpretation is that a tsunamigenic ionospheric hole, a wide depletion of the TEC, occurred after the co-seismic acoustic wave reached the ionosphere and gradually recovered at the normal state within several tens of minutes. The difference between the Heki (2011) and the Kakinami et al. (2012) interpretations is attributed to the different ways in which the TEC reference curves used to extract the ionospheric variations was performed. Another case comes from the analysis of ground based observations. On one side, according to Shestopalov et al. (2013), a precursor to the Chilean earthquake of 27 February 2010 consisted of a significant geomagnetic disturbance observed for about an hour at different magnetic stations of the INTERMAGNET network on February 24, three days before the event, On the other side, Romanova et al. (2015) analyzed in detail data from magnetometers, photometers, and riometers in Canada, Chile, and Antarctica (SAMBA and CARISMA networks). They find that the analysis unambiguously shows that the supposedly anomalous geomagnetic disturbance was not related to seismic activity but instead was caused by a standard isolated substorm.

For some studies on statistics and on mechanisms reported between 2013 and the time of writing a very brief review is given in the Appendix A. This is by no means to be considered as complete.

The purpose of this paper is to report on the analysis of several ionospheric characteristics both observed directly or derived from ionosonde records during two months prior to the 33 h series of very large earthquakes beginning early in the morning of 21 May (Mw = 8.1) and leading to afternoon great Chilean of 22 May 1960 (Mw = 9.5), the largest in recorded history. The analysis can be considered as a follow up to the one reported by Foppiano et al. (2008), which discussed only the critical frequency of the F-region, but using the methodology of Ovalle et al. (2013). The main purpose is again to show whether ionospheric precursors proposed on various statistical studies are consistent with the ones that could be derived for these great Chilean May 1960 earthquakes. The earthquakes are thrust events occurring at a well-defined subduction zones, where the Nazca plate subducts at a rate about 80 mm/yr underneath the South American plate. Most of the fault plane reaches the surface beneath the ocean at several km depths. Detailed reports of this series of earthquakes are given by Cifuentes (1989) and Barrientos and Ward (1990), and the many references within.

2. Data analysis

2.1. Data used

Solar and geomagnetic conditions from 21 March to 21 May 1960 are depicted in Fig. 1 in terms of the solar activity index F10.7 and the geomagnetic activity index Dst, respectively. Solar flare occurrence and characteristics for this interval are given by http://www.ngdc.noaa.gov/stp/space-weather/solar-data/solar-features/solar-flares/h-alpha/tables/1960/. As it can be seen solar activity fluctuates from about 140–200, being highest 1 and 15 April and 11 May, and lowest 21 March, 8, 27 April and 17 May. The geomagnetic activity changes significantly over the same interval. A large geomagnetic storm is observed from 31 March to 10 April which seems to follow a series of flares for which Concepción is on the sunlit hemisphere: 28 March, 15:42–16:44 LT (75°W), importance 2; 29 March, 15:38–16:58, importance 2 and 30 March, 08:55–15:50, importance 1–2+. Between 24 April and 13 May successive depressions of Dst indicate a series of superposed geomagnetic storms.

Values of NmE, NmF2 and NmEs, are derived from observed E-region, F-region and Es critical frequencies over Concepción (36.8°S; 73.0°W), during 21 March–21 May 1960. Although for NmEs determination fbEs (Es blanqueting frequency) should probably be used instead of foEs, this is of no concern for the purpose at hand because finding unusual foEs is easier than fbEs. Diurnal variations of NmE, NmF2 and NmEs are given in Fig. 1 using color codes. In turn, Fig. 2 shows corresponding h'E, h'F and M3000F2 variations. Note that values are depicted at 15 min intervals. However, since for the interval 21 March–30 April only hourly values are available, values at 15 min are interpolated for the presentation's uniformity sake. Since the E-region is not observed using typical ionosondes during night-time, blank spaces are shown in Figs. 1 (NmE) and 2 (h'E) from about 17:00–06:00 LT. Also, there are several blank spaces during daytime. Some of these relate to large Sporadic-E layers below the E-region peak electron concentration, unusual absorption,

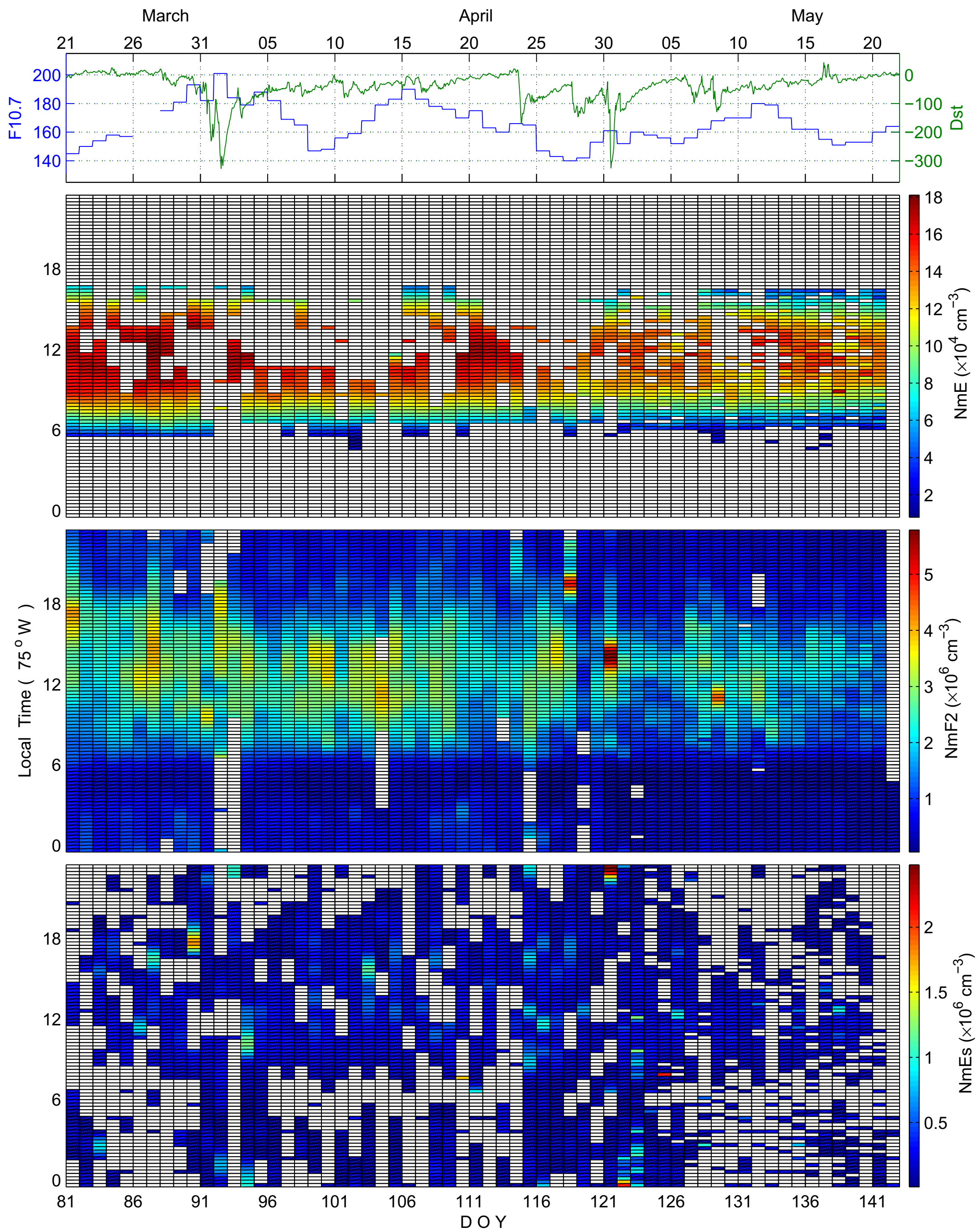

Fig. 1. (top panel) Solar flux F10.7 [10^{-22} Wm^{-2} Hz^{-1}-blue, left scale] and geomagnetic index Dst [nT-green, right scale] for 21 March–21 May 1960 (DOY 81–141). (bottom panels) NmE, NmF2 and NmEs observed over Concepción (36.8°S; 73.0°W).

and occasional radio noise on the lower sounding frequencies.

Diurnal variations of Kp, Dst, foE, foF2, fmin, ftEs (foEs or fxEs when modes identification is not possible), h'E, h'F and M3000F2, together with reference diurnal variations for the ionospheric characteristics, are given in the Supplementary Material for every day from 1 March to 31 May 1960. Reference values correspond to geomagnetically quiet days for each month smoothed using a 3-point mean (7, 13, 20, 22, 23 March; 14, 19, 20, 21, 22 April and 4, 18, 19, 20 May).

2.2. Variability statistics and thresholds

A statistical procedure similar to the one proposed by Chuo et al. (2001) in the case of three earthquakes in Taiwan is used. They determined reference lower boundaries for diurnal variations of foF2 as the running median value

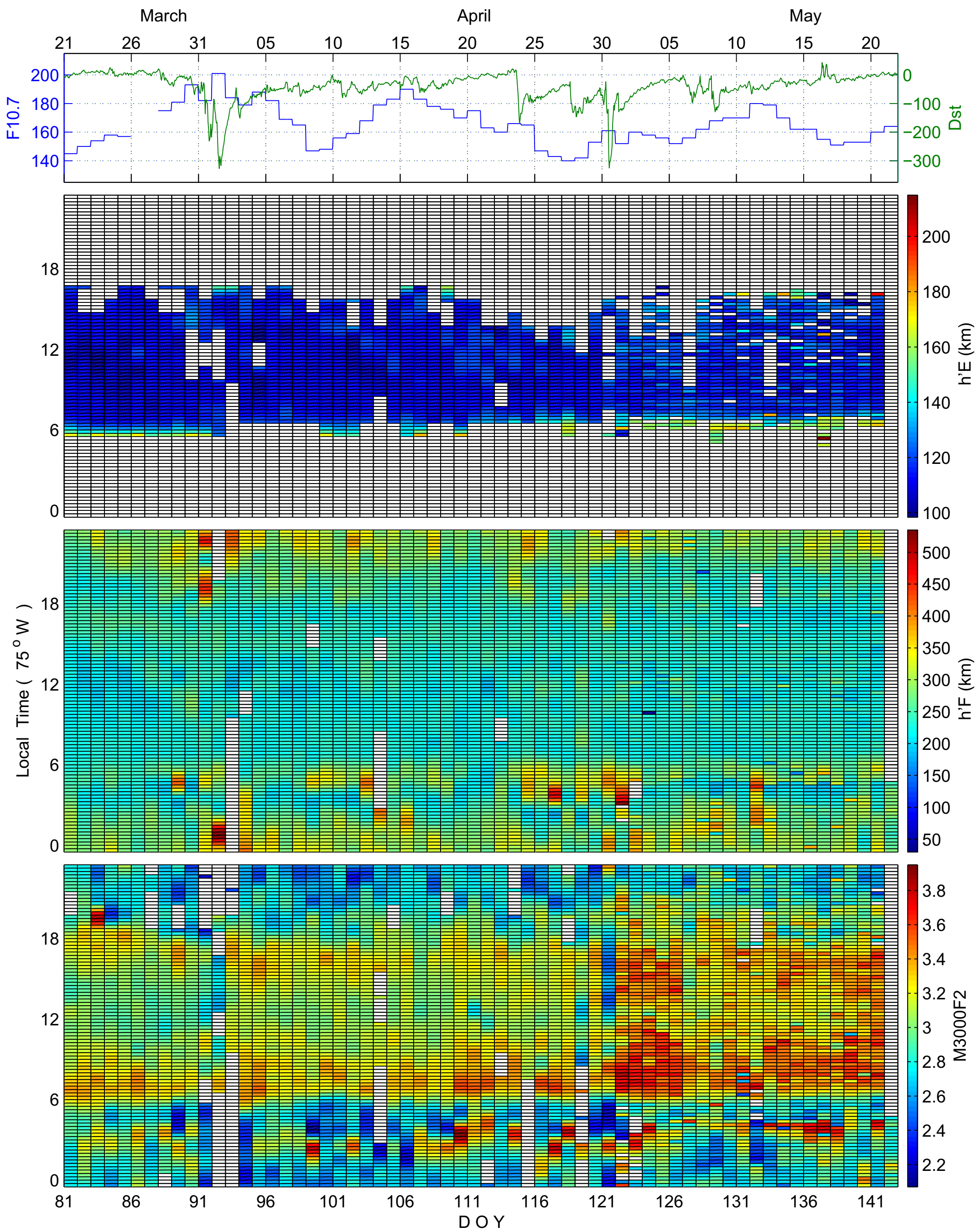

Fig. 2. (top panel) Solar flux F10.7 [10^{-22} Wm^{-2} Hz^{-1}-blue, left scale] and geomagnetic index Dst [nT-green, right scale] for 21 March–21 May 1960 (DOY 81–141). (bottom panels) h'E, h'F2 and M3000F2 observed over Concepción (36.8°S; 73.0°W).

for the last 15 days for a given local time minus the interquartile range. In the present analyses, critical frequencies and electron concentration values are used, and also virtual heights and F-region transmission factor are also considered. Upper and lower reference boundaries are determined as median ± interquartile range. Sample diurnal variations are given in Figs. 3–5. These were selected so as to better show some solar and geomagnetic effects. Occasions when the value of a given characteristic is ⩽the reference lower boundary (LB), ⩾reference upper boundary (UB) and in between LB and UB, using median and interquartile range, are shown in Figs. 6 and 7.

3. Results

3.1. Solar and geomagnetic activity effects

Figs. 1 and 2 show that for several days within the 21 March–21 May some ionospheric characteristics vary differently from the fairly clear diurnal variations corre-

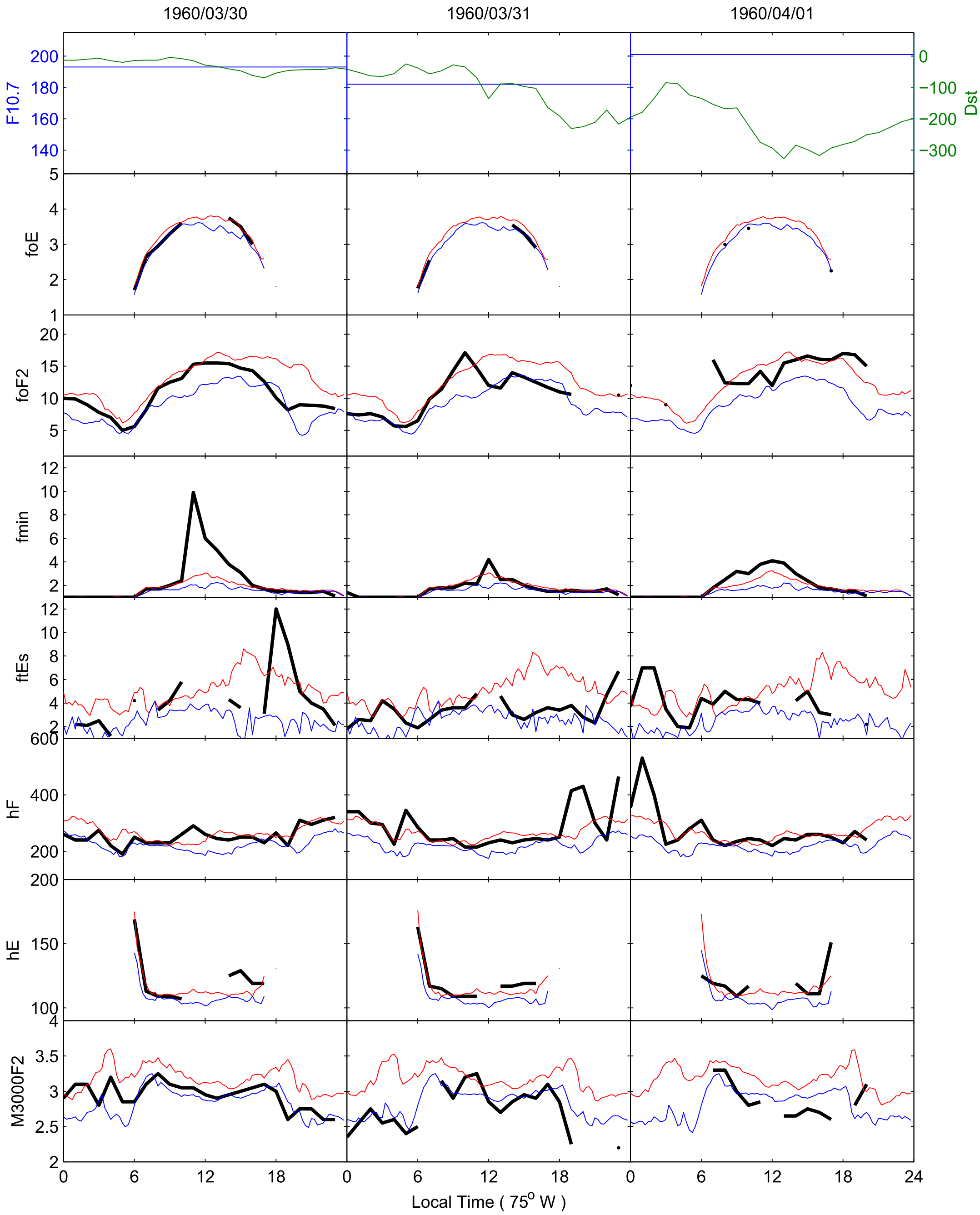

Fig. 3. (from top) Solar flux F10.7 [10^{-22} Wm^{-2} Hz^{-1}-blue, left scale] and geomagnetic index Dst [nT-green, right scale], foE, foF2, fmin and ftEs [MHz], h'F and h'E [km], and M3000F2 for 30 and 31 March and 1 April 1960 (black lines). Reference lower boundary (previous 15-day running median minus interquartile range-blue) and reference upper boundary (previous 15-day running median plus interquartile range-red). (For interpretation of the references to color in this figure legend, the reader is referred to the web version of this article.)

sponding to most days. For example NmF2 is particularly large at certain hours on 21 and 27 March; 9, 13, 26, 27 and 30 April and 8 May. In some cases the increases coincide with large negative excursions of Dst. NmEs, a characteristic that does not follow a regular diurnal variation, is large on 30 March, 30 April and 1 and 4 May. Higher than usual h'F is found more times: 29 and 31 March; 1, 2, 26, 30 April, and 1, 2 and 11 May. So also is M3000F2 on 1 and 30 April, 1–5 and 19 and 20 May.

A detailed analysis of the specific solar and geomagnetic effects for some of the cases is afforded using Figs. 3–5.

On 30 March F10.7 is high (190) and Dst very near to zero. However, following the flares of 28 and 29 March, a series of flares on 30 March from 08:55–15:50 LT, importance 1–2+, are clearly associated with the sudden and large increase of fmin from about 2 MHz to 9.9 MHz and the following exponential decrease reaching quiet level at 16:00, a typical D- and E-region effect. The diurnal

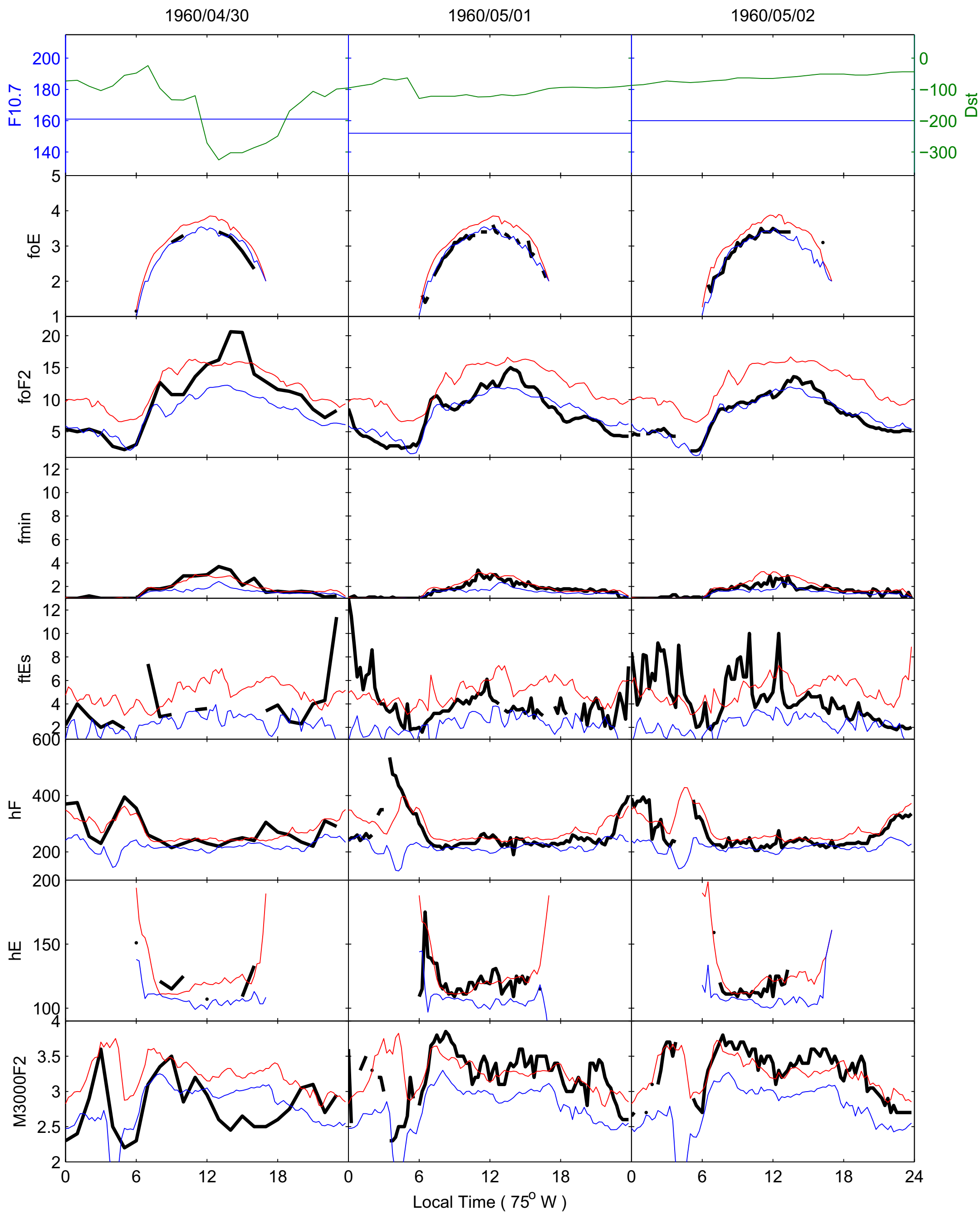

Fig. 4. Same as Fig. 3 for 30 April and 1 and 2 May 1960.

variations of all other characteristics are within the reference boundaries, with the probable exception of ftEs which is much larger than the reference for 18:00 (is 12.0 MHz) and 19:00 LT. Numerical values are not possible from 11:00 to 13:00 for foE, ftEs and h'E most likely due to the large fmin over the time interval. Similar D- and E- effects are seen on 12 May and also on 6 May.

On the following day (31 March) a strong storm (Dst ~ -300 nT) develops. It is probably not associated with the intense flare, importance 3, observed before sunrise or the small flare, importance 1, seen in the morning. Only a small effect on fmin is detected at 12:00, although it is enough to preclude foE and h'E determination at that time. There is a significant increase of foF2 from 09:00 to 11:00. Before and after noon foE cannot be read due to the presence of a blanketing Es layer. At the end of the day Spread F does not permit foF2 and M3000F2 determination, although there is some evidence for very low values of M3000F2 as it was the case also for dawn. The h'F large oscillation at those hours may be doubtful due to Spread F or the rather large ftEs that is observed then; the same is observed on the early hours of the following day (1 April).

fmin is again a bit larger than the upper boundary on 1 April, but this time systematically from about 08:00–15:00.

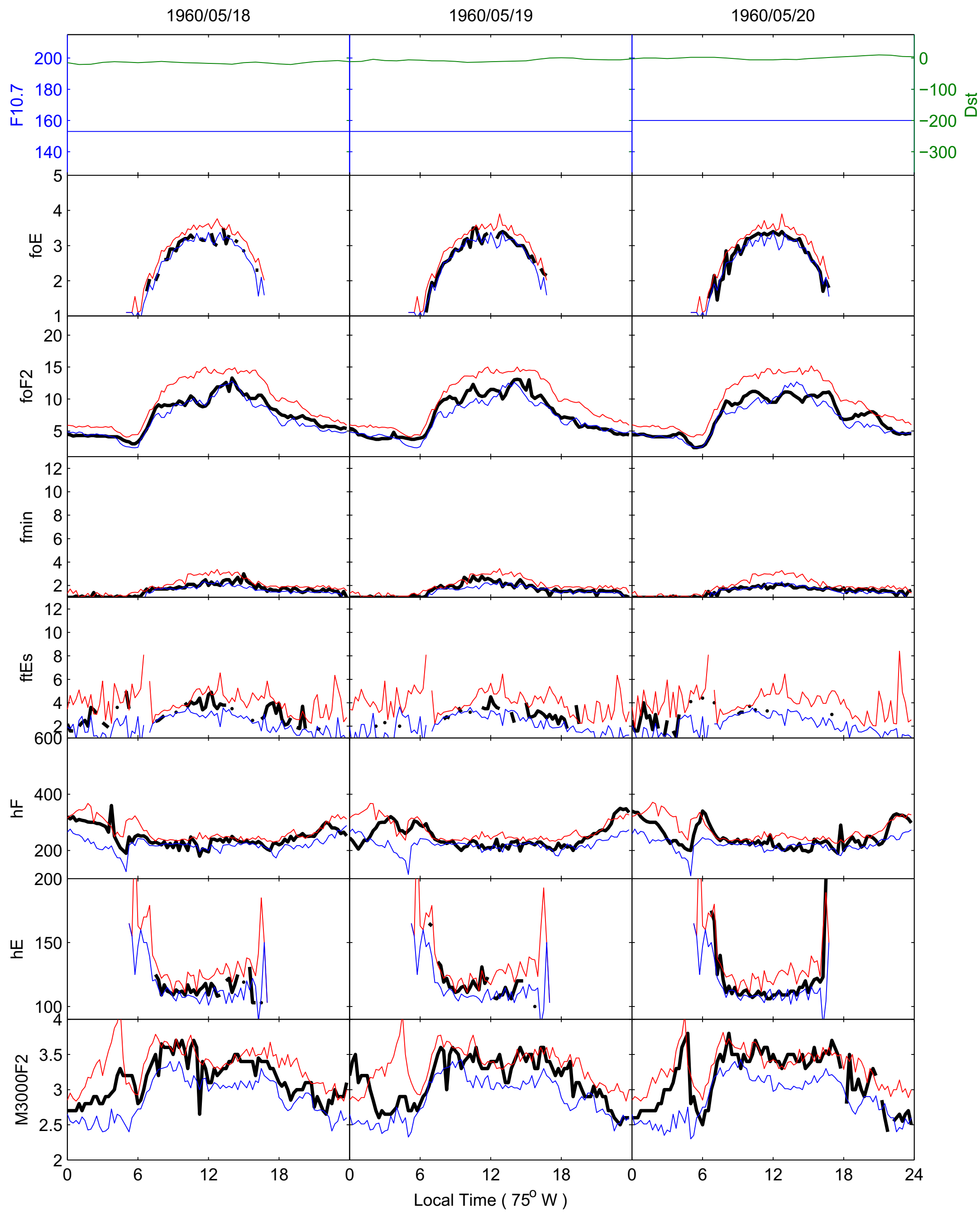

Fig. 5. Same as Fig. 3 for 18, 19 and 20 May 1960.

foE cannot be determined also most of the day. Absorption is evident on ftEs and h'E around noon. Before dawn Spread F continue to be present, thus no foF2 or M3000F2 can be determined. The afternoon clear increase of foF2 and M3000F2 decrease most of the day hours is typical of Concepción F-region storm time (see Arriagada and Foppiano (1999)). The ionosonde observations are not available for three hours before midnight.

Large solar and geomagnetic activities effects are also seen between 24 April and 5 May during a series of successive depressions of Dst, where a magnetic storm does not recover completely before a new one begins. The third and deepest depression starts on the afternoon of 30 April. There are no significant absorption effects in the morning; fmin is only slightly larger than the upper boundary in the afternoon. Some foE values are missing because of absorption as well as a few h'E values; most are related to the presence of Es layers. ftEs is particularly large at 07:00, it is absent due to absorption in the afternoon, and large again just before midnight (11.4 MHz) and the early hours of 1 May, with a typical sudden increase and slowly decrease perhaps more related to chemical developments than to magnetic storm. Again on the 30 April, there are low values of NmF2 and oscillating M3000F2 and h'F

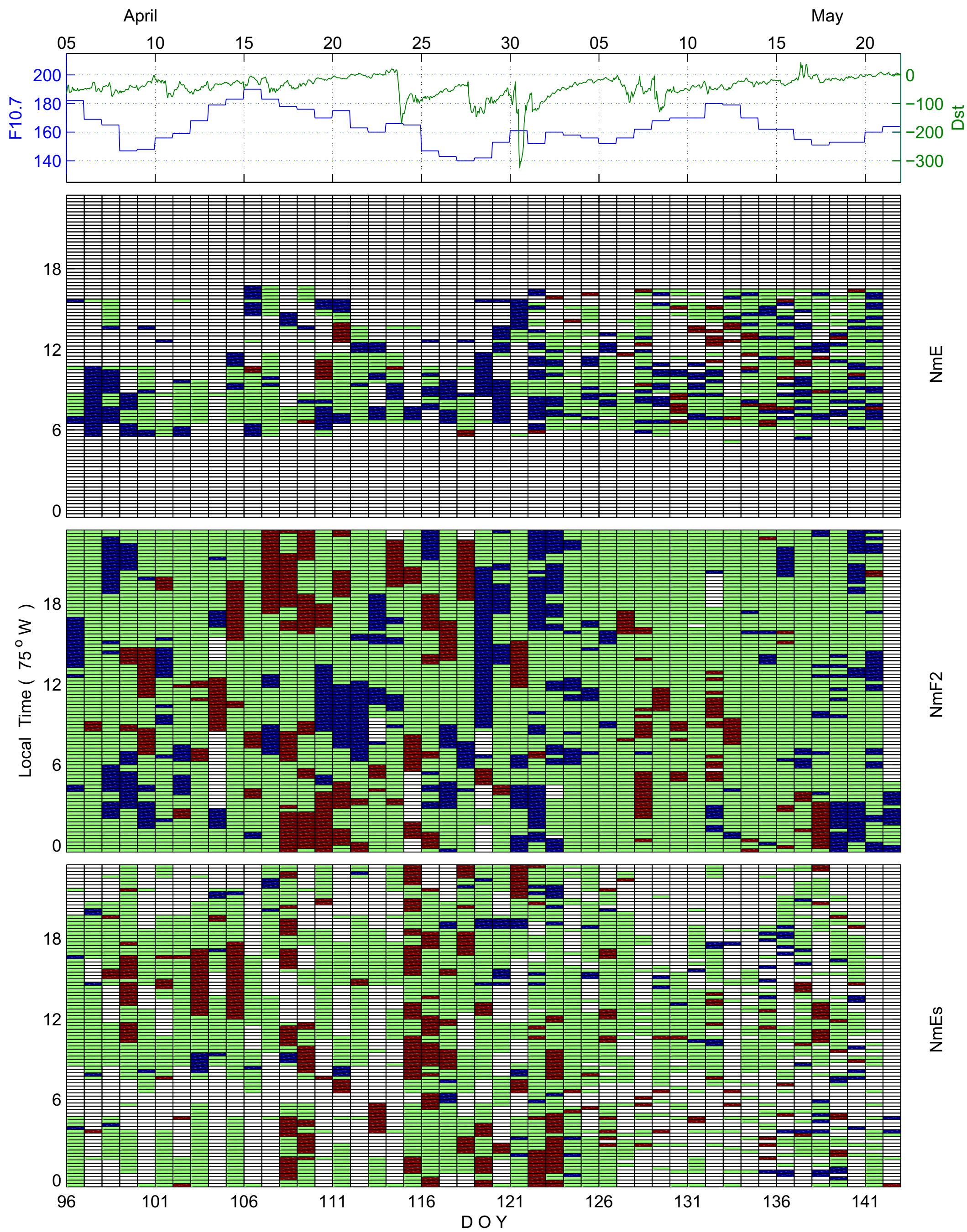

Fig. 6. (top) Same as Fig. 1. Occasions for which NmE, NmF2 and NmEs observed over Concepción (36.8°S; 73.0°W) are ⩽ the reference lower boundary (previous 15-day running median minus interquartile range-blue), ⩾than the reference upper boundary (previous 15-day running median plus interquartile range-red) and in between reference boundaries (green), from 5 April to 21 May 1960 (DOY 96–141). Blank spaces indicate no data.

from midnight to dawn, together with very high NmF2 (∼20.5 MHZ) and low M3000F2 in the afternoon. The abrupt change in the diurnal variation of M3000F2 from 30 April to 1 May could have been considered as an ionospheric precursor. However, this interval is under the effect of strong geomagnetic disturbance. On 2–5 May the geomagnetic disturbance subsides but still large values of M3000F2 are observed (Fig. 2). The M3000F2 factor is related to the shape of the F-region trace on ionograms: the smaller the curvature of the trace the smaller is the factor all other conditions being the same. Smaller (larger) curvature means that electron concentration changes more slowly (faster) with height, thus the factor is related to changes in the height distribution of electron concentration. Observations for several years during late April and early May clearly show the M3000F2 changes semi-annually; with diurnal variations showing two maximum early in the morning and late in the afternoon during

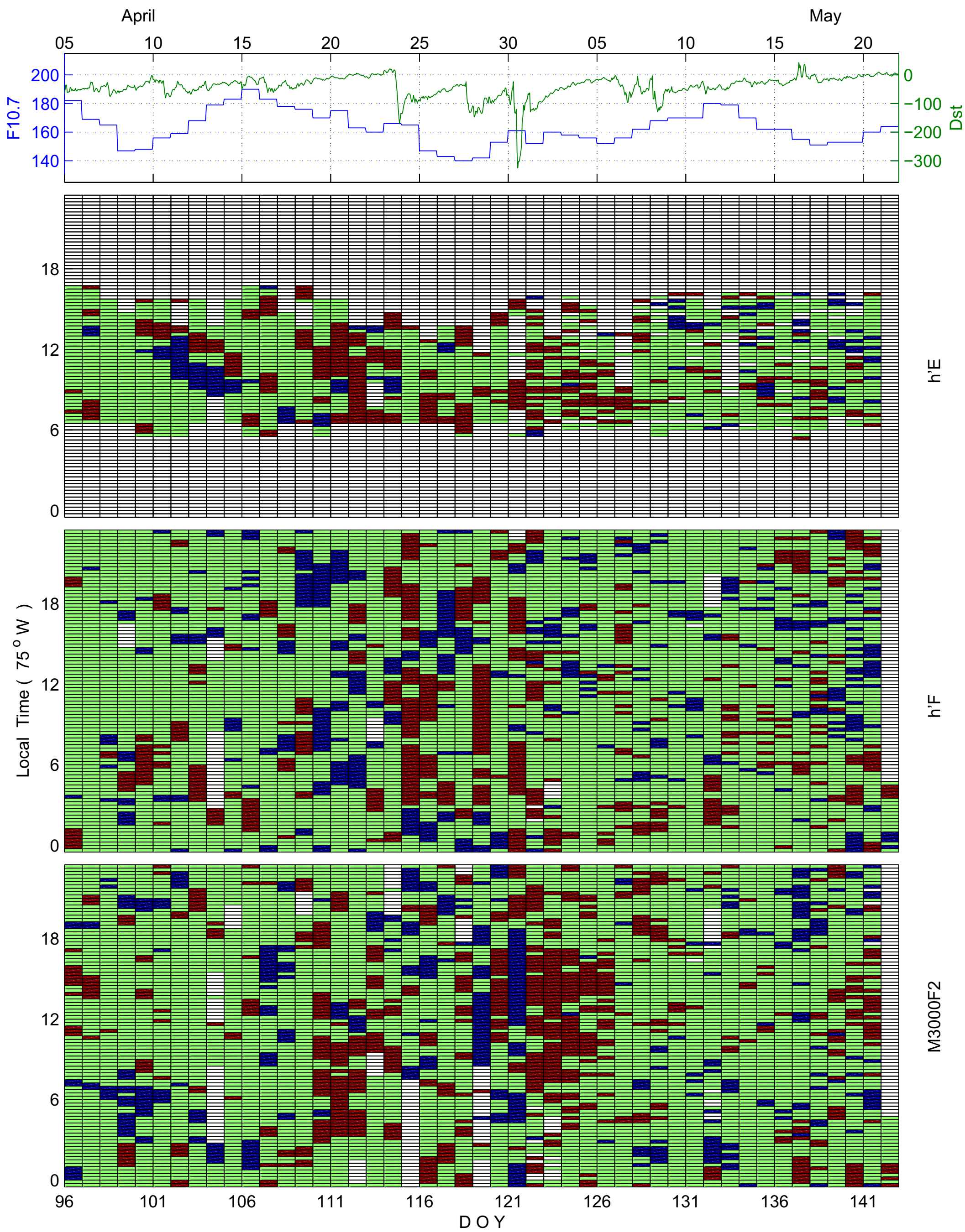

Fig. 7. Same as Fig. 6 but for h'E, h'F2 and M3000F2.

summer, and larger values of the factor in between during autumn and winter. The pattern change from summer/equinox to winter is clearly seen in 1960 after 30 April, probably emphasized by the low values corresponding to large Dst dip of that day. Also, it is recalled that hourly values have been interpolated at 15 min intervals before 1 May and values are actually observed at 15 min intervals after that day. Low M3000F2 values are almost always in relation to magnetic storms. As the storm subsides during 1 and 2 May, simultaneous high ftEs already mentioned and oscillating M3000F2 and h'F are observed; NmF2 is missing from 04:00–04:45 as a result of the large ftEs values, an effect also noticed for M3000F2 and h'F.

A third stormy interval starts on 6 May. Main features are high NmF2 just before noon on 8 May and h'F oscillation between midnight and dawn on 11 May (Supplementary Material).

For time intervals fairly away from storms other effects are also apparent (Figs. 1 and 2). For example, NmEs is very large on 4 May, but lasts less than 30 min. h'F is usually higher before sunrise and after sunset than during daytime. However, larger than usual heights for a few hours are observed 29 March, 12 and 15 April and 11 May. Other instances can be seen in Fig. 5 where detailed diurnal variations are given. Daytime simultaneous oscillations of foF2, M3000F2 and somehow of h'F for 19 and 20 May could be associated with traveling ionospheric disturbances (TIDs). Furthermore, a rather striking effect is the much smaller rate of Es occurrence, particularly on 20 May.

Finally, a simple statistical analysis shows that during the 21 March–20 May interval Spread F occurrence is the same as previously suggested from a climatology for Concepción (Foppiano, 1970).

3.2. Abnormal effects

Occasions for which characteristics are smaller than the LB and larger than the UB, i.e. are abnormal are shown in Figs. 6 and 7.

Fig. 6 shows that NmE values are smaller than LB and larger than UB for about 17% of the time during the 5 April–21 May interval. Do consideration is made that the E-region is visible in the ionograms between about 06:00 and 17:15 LT. Within this interval there are instances (56%) when NmE is not available. NmE smaller than LB occur almost 5 times than values larger than UB.

Fig. 6 also shows that NmF2 values are smaller than the LB and larger than the UB for about 24% of the time during the 5 April–21 May interval. There are some instances (4%) when NmF2 is not available. NmF2 larger than UB occur almost the same number of times than values smaller than LB.

In the case of NmEs values are smaller than the LB and larger than the UB (abnormal values) for about 12% of the time during the 5 April–21 May interval, assuming that an Es layer is always present. NmEs larger than UB occur almost three times than values smaller than LB. This may be due to using foEs instead of fbEs since high foEs values can be related to oblique echoes or Es layer patchiness (Lăstovička et al., 2012). In any case, the argument for possible precursors is not hindered by this fact.

Fig. 7 shows that h'E values are smaller than the LB and larger than the UB (abnormal values) for about 20% of the time during the 5 April–21 May interval. Do consideration is made that the E-region is visible in the ionograms between about 06:00 and 17:15 LT. Within this interval there are some instances (39%) when h'E is not available. h'E larger than UB occur almost 3 times than values smaller than LB.

Fig. 7 also shows that h'F values are smaller than the LB and larger than the UB (abnormal values) for about 23% of the time during the 5 April–21 May interval. There are some instances (5%) when h'F is not available. h'F larger than UB occur almost the same number of times than values smaller than LB.

In the case of M3000F2 values are smaller than the LB and larger than the UB (abnormal values) for about 25% of the time during the 5 April–21 May interval. There are some instances (8%) when M3000F2 is not available. M3000F2 larger than UB occur almost twice the number of times than values smaller than LB.

In the case of the 27 February 2010 earthquake (27/F) very similar results for NmF2 were obtained: larger and smaller than thresholds about the same percentage of time and number of times larger than UB almost the same than smaller than LB.

Moreover, NmF2 higher than the UB is much more frequent than NmF2 lower than the LB when F10.7 is relatively high, as it was the case for the 27/F. So also NmF2 lower than the LB is less frequent than NmF2 higher than UB, again consistent with the 27/F case.

Once again, instances for NmF2 smaller than LB are more frequent during a few days prior the Chilean May 1960 earthquake as it was found for the 27/F.

From 2 May-5 May and again from 18 to 20 May values of M3000F2 are larger than the UB around midday. Is this a possible precursor? New scaling of January and February 2010 ionograms shows the typical summer diurnal variation of M3000F2. Unfortunately, there are many hours for which no data is available just around midday, precluding a firm conclusion to be made.

4. Discussion

The results for NmF2 found in the present study are similar to the ones already discussed when reporting on the Chilean 27 February 2010 (Ovalle et al., 2013). Thus, no detailed discussion on this ionospheric characteristic in relation of published results generally available till about July 2013 is given. The conclusion then and now is that the results are consistent with some published reports and definitely not consistent with others.

Work published after July 2013, related to TEC studies using traditional and more sophisticated techniques for earthquakes in China, Japan, Uzbekistan, Chile (Iquique 2014), Samoa and Haiti are also not discussed here. These are only briefly commented upon in the Appendix A because no TEC observations were possible during 1960. For the same reason no newer satellite results are considered. Neither are new results on unusual animal behavior also quoted in the Appendix A.

Here some detailed Es characteristics comparisons are made with published results. There are five occasions for which ftEs $\geqslant$ 10 MHz (30 March, 30 April, 1 and 4 May). For these, mean fbEs is 5.2 MHz and mean difference (ftEs–fbEs) is 7.0 MHz. Reference average monthly mean ftEs and fbEs are 3.1 and 1.7 MHz, with upper and lower quartiles of 4.2, 2.2 and 2.1, 1.5 MHz for ftEs and fbEs, respectively. Thus, the high quoted values for ftEs and fbEs are indeed abnormal. Similar results are found for eight occasions on the same days for which ftEs < 10.0 but larger than normal: mean fbEs = 2.9, mean difference = 2.9, average monthly means = 2.5 and 1.3 MHz, for ftEs and fbEs, respectively. Moreover, a simple Es statistics for all 1960 months shows a clear annual variation of Es occurrence: the number of events with continuous Es occurrence for at least 2 h (ftEs ⩾ than the reference) is largest during summer and smallest in winter (19 and 7); intermediate during equinox (11). The May occurrence is twice as expected from this annual variation and there are more events before the earthquake than after it, the lack of observations for 5 days after being considered. But, on 17 May (4 days before the earthquake onset) there is the same number of events than on 1, 2 and 5 May, thus reducing the likelihood of this being an ionospheric precursor.

Regarding historical high values of foEs a warning form Lăstovička et al. (2012) is worth considering. They analyzed 282 events (hourly values) of high foEs ⩾ 6 MHz observed by the digisonde DPS-4 at Pruhonice (49°59’N, 14°33’E) over the period 2004–2010. They find that 90% of "classic" ionosonde high foEs are over-estimated by 0.1–3.4 MHz compared to the "true" foEs from digisonde; about 38% of high "classical" foEs values are oblique reflections with deviations from vertical by 15–45°; the diurnal variation of occurrence frequency of high foEs roughly corresponds to the solar zenith angle variation of electron density in the E-layer – an unexpected and very strong year-to-year variation of occurrence of high foEs was observed though.

Parrot and Mogilevsky (1989) analysed foEs observations at Djibouti station (110°N; 42°E) for several earthquakes in 1978, 79 and 80. Records were made every 15 min. Monthly mean foEs ± standard deviation was used as variability measure. They find that for several cases, foEs was larger than the variability within a few hours of the earthquakes. However, the same was found to be true for times after the earthquakes. The main results quoted by Parrot et al. (1993) in their review of on ionospheric perturbations observed using ionosondes are that nocturnal anomalies in the Es regions do exist: diffusion and quick decrease of foEs two days before earthquakes in Russia (Alimov et al., 1989), and Es layers formation during the night preceding the Chilean 1960 earthquake at distances larger than 2500 km (Gokhberg et al., 1989).

Liperovsky et al. (2000) have extensively reviewed E-region detailed effects reportedly caused by earthquakes using a Russian network of ground based ionospheric stations. The stations are situated at distances of some hundreds of kilometers from one to another and operated over several years. Main attention is paid to sporadic E-layers. Results are for some 700 nights. For Es layers lasting a few hours and earthquakes of magnitude $M \geqslant 5.0$ at distances $R < 500$ km from the stations, fbEs during the night previous to the earthquake decreases relative to the night before that. No decrease of the average fbEs for both nights was found for the earthquakes with $M < 5.0$. For shorter Es layers, the number of bays (differences from earlier and later steady levels) per night with shortest time scale (<0.5 h) has a tendency to decrease during seismo-active nights in comparison with the background nights, the ones with scales between 2 and 3 h have a tendency to increase, and for those of 0.75–2 h, the averaged number is almost the same for seismo-active and background nights. For the shortest lasting Es layers fbEs variability increases during the first and second nights before the earthquakes.

Anomalous foEs before the Hyogo-ken Nambu 17 January 1995 earthquake in Japan have been reported by Ondoh (2003). He finds that daytime foEs increased to over 8.0 MHz during 2 days before the earthquake at Shigaraki, relatively near the epicentre (about 120 km) and also up to 9.0 MHz 5 days before at Kokubunji, some 500 km away from it. No such high values were observed at other three ionosondes which are further away from the epicentre. Geomagnetic activity was quiet during 6 days before the earthquake according to Kakioka geomagnetic station (local K indices mostly below 3) and no solar events or increased fluxes (F10.7) were observed. Monthly median daytime foEs values during winter over the five ionospheric stations are quoted to be below 6 MHz. Thus, the high foEs values were regarded as ionospheric seismic precursors.

Liperovsky et al. (2008) suggest that when considering seismo-ionospheric effects in the E- region Es-spread and layer semi-transparency ((foEs–fbEs)/fbEs) should be checked. They report that the day before the earthquake Es-spread intensifies and semi-transparency decreases. Here, the checking was done for three days before the 21–22 May earthquakes. It is found that only a very limited Es-spread occurs on 20 May from 00:30 to 02:15 LT. This cannot be considered as abnormal for the Equinox/Winter season. As per the semi-transparency, this clearly increases during daytime (from about 0.2–1.4) and slightly decreases at night-time (0.8–0.7) on 20 May in relation to 19 May. No ionograms are available after 06:00 for four days due to power failure.

As already mentioned, the M3000F2 diurnal variation pattern is seen to change between 30 April and 1 May. This could have been considered as an ionospheric precursor, since the factor is related to a possible redistribution of electron concentration. Unfortunately, there seem to be no other specific studies of M3000F2 so as to confirm this feature.

Finally, it is recalled that Kuo et al. (2014) has proposed theoretical modeling which relates surface charges buildup over stressed rock and nearby air based on seismic active areas with changes on ionospheric dynamic. This modeling suggests the effects of atmospheric currents and electric fields on the ionosphere thus produced are strongly dependent on lithosphere current-source magnetic latitudes (see Appendix A). This means that either increases or decreases of total electron content (TEC) can arise on contiguous narrow latitude ranges. This may explain the diverse results obtained from different studies, including the present one: it would depend on whether Concepción is on an upward or downward current (decrease or increase of TEC) within the 22.5–30° magnetic latitude range. As discussed for other TEC studies, no TEC determinations are possible for the 1960 Chilean earthquake.

However, the quoted model also suggest that ionospheric bubbles may arise over the magnetic flux lines starting from lithosphere/ground surface charge build up. If these bubbles are responsible for equatorial Spread-F occurrence, Concepción ionosonde observations may be used to detect this phenomenon since the magnetic latitude of Concepción is 22°S. The simple counting of Spread-F occurrence during 21 March–20 May 1960 shows that almost all events occur between 00:00 and 08:00 LT. Significant events, lasting more than 4 h, are found on 1, 2, 3 and 24 April and 1 May. All cases correspond to magnetic storm conditions and thus could be hardly unambiguously associated with lithospheric/ground signals.

5. Conclusions

This study seems to be the first to consider simultaneous E- and F-region characteristics observed at Concepción (36.8°S; 73.0°W) using a ground based ionosonde prior to the very large Chile earthquakes of 21–22 May 1960.

An analyses of NmE, NmEs, h'E, NmF2, h'F, M3000F2 and fmin is offered taking into account possible solar and geomagnetic activity effects.

Occasions when anomalies are larger than an upper threshold and less than a lower threshold are discussed and compared, whenever possible, with other published studies.

The results for NmF2 are similar to the ones already discussed when reporting on the Chilean 27 February 2010 (Ovalle et al., 2013). The conclusion then and now is that the results are consistent with some published reports and definitely not consistent with others.

The M3000F2 diurnal variation pattern is seen to change between 30 April and 1 May. This could have been considered as an ionospheric precursor, since the factor is related to a possible redistribution of electron concentration. Unfortunately, it was not possible to separate this effect from known seasonal variation. Furthermore, there seem to be no other specific studies of M3000F2 so as to confirm this feature.

Further study is suggested to unambiguously associate some found possible Es-layer anomalies with very strong earthquakes.

Acknowledgements

We are indebted to the engineers and technicians who operated the Concepción C4 and IPS 42 ionosondes for over 50 years; without their endeavours the present report and the previous ones on the 1960 and 2010 Chilean earthquakes would have been impossible. In particular, to the late Harald Sagner, Carlos Figueroa and also the late Avelino Saez, the latter diligently scaled most ionograms. Comments received from Inez S. Batista and from other referee that led to significant text changes are most welcomed.

Appendix A

More statistical studies for over 200 earthquakes in China and Japan have been carried out by Liu et al. (2013a,b). Precursors of the total electron content (TEC) in the global ionosphere map (GIM) associated with 146 $M \geqslant 6.0$ earthquakes in Japan during 14 May 1998–31 July 2011 and with 56 $M \geqslant 6.0$ in China during 1998–2012 are considered. To detect TEC precursors median plus quartiles are calculated. The earthquakes are sub-divided into 3 regions to better identify precursor characteristics. Magnetic storms intervals are excluded. It is found precursors consist of significant TEC increases in the afternoon, 1–5 days before earthquakes in Japan and decreases, 2–9 days before the earthquakes in China. Furthermore, analysis of TEC for two Uzbekistan stations are given by Tojiev et al. (2013) using a differential TEC as obtained by subtracting monthly averaged diurnal TEC from the values of observed vertical TEC at each epoch. The results show anomalous increase or decrease of TEC 1–7 days before earthquakes. Some statistical studies emphasize the use of multiple instrument observations both ground-based and space-borne (e.g. infrared radiation, TEC and NmF2 as in Ouzounov et al. (2011)).

In a series of papers searching also for TEC precursors but for selected recent large earthquakes (Iquique, Tohoku, Samoa, Haiti) Akhoondzadeh (2012, 2013a, 2013b and 2014) has used somehow more sophisticated analyses than standard mean or median statistics. He uses wavelet transforms, Auto-Regressive Integrated Moving Average, Kalman filters, computational-intelligence genetic algorithms and multi-layer perceptron (MLP) neural networks. In most cases, similar results are found, namely TEC anomalies one to five days before earthquake onset (7–8 days for Samoa) depending on the earthquake and geomagnetic activity level (as measured by Dst index). He finds the MLP analysis a promising technique as it better relates to non-parametric/non-linear phenomena.

A completely different approach, developed during last few years, is the one of Li and Parrot (2013). Instead of searching for anomalies prior to some specific earthquakes, they assemble anomalies world-wide and try to determine the location and timing of earthquakes. Ion density was recorded by the low-altitude satellite DEMETER during more than 6 years, and a search for anomalies was automatically conducted with the complete data set. Then, some software is used to check if a given anomaly could correspond to an earthquake: distances less than 1500 km from the anomaly positions and times up to 15 days after anomaly time were considered. Earthquakes were selected according to magnitude, depth, and position (below the sea or inland). They find that: the percentage of good detections always increases with earthquake magnitude; on average, the amplitude of the perturbations is related to the earthquake magnitude and the number of perturbations is higher on the earthquake occurrence day, the percentage gradually decreasing for longer intervals; there are seismic areas on the Earth's surface where it is possible to use the technique because natural ionospheric perturbations is too large (e.g. South Atlantic Magnetic Anomaly); earthquakes over sea are better detected than over land. Detection examples shown are for the Mw 8.8 Chile 27 February 2010 and the Mw 6.3 Pacific 19 November 2007 earthquakes. Determined earthquake locations are within ±12° latitude and ±15° longitude for the Chilean earthquake and slightly larger for the Pacific one.

Satellite quasi-static electric fields observations have also been recently reported in relation to earthquake precursors (Zhang et al. 2014). They present ULF electric field (DC-15 Hz) observations by the DEMETER satellite over two seismic regions of Indonesia and Chile. Three-component electric field data were collected along all the up-orbits (in local nighttime) at distances less than 2000 km from the epicenters for 9 and 7 days before and 1 day after the earthquakes. For all the 57 perturbations found the amplitude of quasi-static electric field perturbations varies from 1.5 to 16 mV/m in the upper ionosphere, most being less than 10 mV/m. Among all 27 cases, for 10 earthquakes the perturbations occur just one day prior to the earthquake. Perturbations are more frequent in the Chilean case.

Grant and Conlan (2015) quote unusual behavior prior to earthquakes that has been reported for millennia, although most reports are classified as anecdotal, and also some systematic evaluations of animal behavior changes prior to earthquakes for which behavior has been recorded in a methodical way. Moreover, they set up experiments that confirm the specific behaviors of some animals in the presence of hydrogen peroxide, which is also generally associated with chemical and physical water properties at large. They follow the proposed mechanism developed by Freund over several year and recently summarized (Freund, 2013). This mechanism relates to the air ionization on the ground-air interphase. Metastable peroxy defects in minerals in igneous and high-grade metamorphic rocks, which release highly mobile electronic charge carriers, when the rocks are subjected to mechanical stress. Those charge carriers consist of defect electrons in the oxygen anion sublattice. Known as "positive holes", they are associated with energy states at the upper edge of the valence bands. The upward migration of positive oxygen ions could reach ionospheric heights thus leading to an electron concentration redistribution which could produce some type of seismic associated anomaly. The proposed ionization mechanism would be also related to other unusual animal behavior as reported recently (e.g. Fidani et al. (2014)).

Assuming the buildup of surface charges over the stressed rock and in the nearby air based on seismic active areas as suggested by Freund, Kuo et al. (2014) recently up dated a quantitative model. This first gives the surface charge density and electric field at the ground-to-atmosphere interface. Then the current continuity equation is used to calculate the current density and electric fields in the atmosphere, and finally the 3D SAMI3 model is used to examine the ionosphere dynamics. The effects of atmospheric currents and electric fields on the ionosphere with lithosphere current source located at magnetic latitudes of 7.5°, 15°, 22.5°, and 30° are obtained. For upward (downward) atmospheric currents flowing into the ionosphere, the simulation results show that the westward (eastward) electric fields dominate. At magnetic latitude of 7.5° or 15°, the upward (downward) current causes the increase (decrease) of total electron content (TEC) near the source region, while the upward (downward) current causes the decrease (increase) of TEC at magnetic latitude of 22.5° or 30°. They also calculate the ionosphere dynamics with imposed zonal westward and eastward electric field based on SAMI3 code. It is found that the eastward (westward) electric field may trigger one (two) plasma bubble(s) in the nighttime ionosphere.

On the possible development of detection and monitoring of earthquake precursors Chmyrev et al. (2013) proposes and early warning system using coordinated satellite and ground-based observations. The mission would consist of two co-orbit satellites separate by some 400 km. The proposed observations are as follows. TwinSat M: DC electric field vector; spectral and wave characteristics of 6 electromagnetic field components in ULF/ELF range (0.5–500 Hz); spectrum and sample waveforms of electric field oscillations in VLF/LF (0.5–300 kHz) range; amplitude and phase variations of ground based VLF/LF transmitter signals; spectrum and sample waveforms of electromagnetic waves in VHF range (22–48 MHz); variations of thermal and supra thermal (0.3–20 eV) plasma parameters; energy distributions of electron and ion fluxes with energies 3–300 eV for two directions. TwinSat: variations of thermal and supra thermal (0.3–20 eV) plasma parameters; energy distributions of electron and ion fluxes with energies 0.3–300 eV for two directions; wave form of ULF/ELF magnetic field oscillations (0.5–500 Hz), one or two components. Other satellites: spatial strain maps of potential earthquake areas from InSAR data; outgoing IR (8–12.5 μm) radiation intensity and thermal images of seismically active zones; space weather monitoring to be able to take account of magnetospheric effects. Ground-based: atmospheric gas composition; radon emission and variations of radioactivity; dynamics of aerosol injection; atmospheric DC electric field and current variations; spectral and wave characteristics of ULF/ELF/VLF/VHF electromagnetic emissions including the arrival direction finding and locating the radiation sources; remote sensing of ionospheric disturbances through the registration of amplitude and phase variations of VLF/LF signals from ground-based transmitters at appropriate propagation routes; debit, temperature and chemical composition of underground water sources and holes; air temperature and humidity, wind velocity and atmospheric pressure; seismic and magnetic field oscillations.

Appendix A. Supplementary data

Supplementary data associated with this article can be found, in the online version, at http://dx.doi.org/10.1016/j.asr.2015.09.015.

References

Akhoondzadeh, M., 2012. Anomalous TEC variations associated with the powerful Tohoku earthquake of 11 March 2011. Nat. Hazards Earth Syst. Sci. 12, 1453–1462.

Akhoondzadeh, M., 2013a. Support vector machines for TEC seismo-ionospheric anomalies detection. Ann. Geophys. 31, 173–186.

Akhoondzadeh, M., 2013b. Genetic algorithm for TEC seismo-ionospheric anomalies detection around the time of the Solomon (Mw = 8.0) earthquake of 06 February 2013. Adv. Space Res. 52, 581–590.

Akhoondzadeh, M., 2014. Investigation of GPS-TEC measurements using ANN method indicating seismo-ionospheric anomalies around the time of the Chile (Mw = 8.2) earthquake of 01 April 2014. Adv. Space Res. 54, 1768–1772.

Alimov, O.A., Gokhberg, M.B., Liperovskaya, E.V., Gufeld, I.L., Liperovsky, V.A., Roubtov, L.N., 1989. Anomalous characteristics of the middle latitude Es layer before earthquakes. Phys. Earth Planet. Inter. 57, 76–81.

Arriagada, M.A., Foppiano, A.J., 1999. Algoritmo para completar series de valores de la frecuencia crítica de la región F de la ionósfera sobre Concepción. Rev. Bras. Geofís. 17, 13–20.

Barrientos, S.E., Ward, S.N., 1990. The 1960 Chile earthquake; inversion for slip distribution from surface deformation. Geophys. J. Int. 103, 589–598.

Biagi, P.F., Contadakis, M.E., Hayakawa, M., Maggipinto, T. (Eds) 2012. Earthquake precursor research: ground-satellite observations, laboratory experiments, and theoretical models. Ann. Geophys. 55 (Special Issue).

Chuo, Y.J., Chen, Y.I., Liu, J.Y., Pulinets, S.A., 2001. Ionospheric foF2 variations prior to strong earthquakes in Taiwan area. Adv. Space Res. 27, 1305–1310.

Chmyrev, V., Smith, A., Kataria, D., Nesterov, B., Owen, C., Sammonds, P., Sorokin, V., Vallianatos, F., 2013. Detection and monitoring of earthquake precursors: TwinSat, a Russia-UK satellite project. Adv. Space Res. 52, 1135–1145.

Cifuentes, I.L., 1989. The 1960 Chilean earthquake. J. Geophys. Res. 94, 665–680.

Fidani, C., Freund, F., Rachel Grant, R., 2014. Cows come down from the mountains before the (Mw = 6.1) earthquake Colfiorito in September 1997; a single case study. Animals 4, 292–312.

Foppiano, A.J., 1970. Spread-F. Principales variaciones del fenómeno de dispersión de ondas electromagnéticas por la región F de la ionósfera sobre Concepción (Thesis submitted to apply for the Mathematics and Physics Teacher (secondary school) title). Universidad de Concepción, Concepción, Chile.

Foppiano, A.J., Ovalle, E.M., Bataille, K., Stepanova, M., 2008. Ionospheric evidence of the May 1960 earthquake over Concepción? Geofís. Int. 43, 179–183.

Forbes, J.M., Palo, S.T., Zhang, X., 2000. Variability of the ionosphere. J. Atmos. Solar Terr. Phys. 62, 685–693.

Freund, F., 2013. Earthquake forewarning-a multidisciplinary challenge from the ground up to space. Acta Geophys. 61, 775–807.

Grant, R.A., Conlan, H., 2015. Behavioral response of invertebrates to experimental simulation of pre-seismic chemical changes. Animals 5, 206–213.

Gokhberg, M.B., Ustov, A.V., Liperovaskiy, V.A., Liperovskaya, R.K. H., Kharin, E.P., Shalimov, S.L., 1989. Perturbations of the ionospheric F-layer prior to strong prior to strong earthquakes. Izv. Earth Phys. 24, 254–260.

Heki, K., 2011. Ionospheric electron enhancement preceding the 2011 Tohoku-Oki earthquake. Geophys. Res. Lett. 38, L17312. http://dx.doi.org/10.129/2011GL047908.

Kakinami, Y., Kamogawa, M., Tanioka, Y., Watanabe, S., Gusman, A. R., Liu, J.-Y., Watanabe, Y., Mogi, T., 2012. Tsunamigenic ionospheric hole. Geophys. Res. Lett. 39, L00G27. http://dx.doi.org/10.1029/2011GL050159.

Kamogawa, M., Kakinami, Y., 2013. Is an ionospheric electron enhancement preceding the 2011 Tohoku-Oki earthquake a precursor? J. Geophys. Res. 118, 1751–1754.

Kuo, C.L., Lee, L.C., Huba, J.D., 2014. An improved coupling model for the lithosphere–atmosphere–ionosphere system. J. Geophys. Res. 119, 3189–3205.

Lăstovička, J., 2006. Forcing of the ionosphere by waves from below. J. Atmos. Sol. Terr. Phys. 68, 479–497.

Lăstovička, J., Bǒska, J., Burěsová, D., Kouba, D., 2012. High historical values of foEs—reality or artefact? J. Atmos. Sol. Terr. Phys. 74, 51–54.

Li, M., Parrot, M., 2013. Statistical analysis of an ionospheric parameter as a base for earthquake prediction. J. Geophys. Res. 118, 3731–3739.

Liperovsky, V.A., Pokhotelov, O.A., Liperovskaya, E.V., Parrot, M., Meister, C.-V., Alimov, O.A., 2000. Modification of sporadic *e*-layers caused by seismic activity. Surv. Geophys. 21, 449–486.

Liperovsky, V.A., Pokhotelov, O.A., Meister, C.V., Liperovskaya, E.V., 2008. Physical models of coupling in the lithosphere–atmosphere–ionosphere system before earthquakes. Geomag. Aeron. 48, 795–806.

Liu, J.Y., Chen, C.H., Tsai, H.F., 2013a. A statistical study on seismo-ionospheric precursors of the total electron content associated with 146 M $\geqslant$ 6.0 earthquakes in Japan during 1998–2011. In: Hayakawa, M. (Ed.), Earthquake Prediction Studies: Seismo Electromagnetics. TERRAPUB, Japan, pp. 1–13.

Liu, J.Y., Chen, C.H., Tsai, H.F., Le, H., 2013b. A statistical study on seismo-ionospheric anomalies of the total electron content for the period of 56 M $\geqslant$ 6.0 earthquakes occurring in China during 1998–2012. China J. Space Sci. 33, 258–269.

Mendillo, M., Rishbeth, H., Roble, R.G., Wroten, J., 2002. Modelling F2-layer seasonal trends and day-to-day variability driven by coupling with the lower atmosphere. J. Atmos. Sol. Terr. Phys. 64, 1911–1931.

Ondoh, T., 2003. Annomalous sporadic-E layers observed before M 7.2 Hyogo-ken Nanbu earthquake; terrestrial gas emanation model. Adv. Polar Upper Atmos. Res. 17, 96–108.

Ouzounov, D., Pulinets, S., Romanov, A., Romanov, A., Tsybulya, K., Davidenko, D., Kafatos, M., Taylor, P., 2011. Atmosphere–ionosphere response to the *M*9 Tohoku earthquake revealed by multi-instrument space-borne and ground observations: preliminary results. Earthquake Sci. 24, 557–564.

Ovalle, E.M., Bravo, M.A., Villalobos, C.U., Foppiano, A.J., 2013. Maximum electron concentration and total electron content of the ionosphere over Concepción, Chile, prior to the 27 February 2010 earthquake. Adv. Space Res. 52, 1274–1288.

Parrot, M., Mogilevsky, M.M., 1989. VLF emissions associated with earthquakes and observed in the ionosphere and the magnetosphere. Phys. Earth Planet. Inter. 57, 86–99.

Parrot, M., Achache, J., Berthelier, J.J., Blanc, E., Deschamps, A., Lefeuvre, F., Menvielle, M., Plantet, J.L., Tarits, P., Villain, J.P., 1993. High-frequency seismo-electromagnetic effects. Phys. Earth Planet. Inter. 77, 65–83.

Pulinets, S.A., 2007. Natural radioactivity, earthquakes, and the ionosphere. EOS, Trans. Am. Geophys. Union 88, 217–224.

Pulinets, S.A., Boyarchuk, K.A., 2004. Ionospheric Precursors of Earthquakes. Springer, New York (p. 315).

Pulinets, S., Davidenko, D., 2014. Ionospheric precursors of earthquakes and global electric circuit. Adv. Space Res. 53, 709–723.

Rishbeth, H., 2007. Do earthquake precursors really exist? EOS, Trans. Am. Geophys. Union 88, 296.

Romanova, N.V., Pilipenko, V.A., Stepanova, M.V., 2015. On the magnetic precursor of the Chilean earthquake of February 27, 2010. Geomag. Aeron. 55, 219–222.

Shahrisvand, M., Akhoondzadeh, M., Sharifi, M.A., 2014. Detection of gravity changes before powerful earthquakes in GRACE satellite observations. Ann. Geophys. 57, A0543. http://dx.doi.org/10.4401/ag-6612.

Shestopalov, I.P., Belov, S.V., Soloviev, A.A., Kuzmin, Yu.D., 2013. Neutron generation and geomagnetic disturbances in connection with the Chilean earthquake of February 27, 2010 and a volcanic eruption in Iceland in March–April 2010. Geomag. Aeron. 53, 124–136.

Tojiev, S.R., Ahmedov, B.J., Tillayev, Y.A., Eshkuvatov, H.E., 2013. Ionospheric anomalies of local earthquakes detected by GPS TEC measurements using data from Tashkent and Kitab stations. Adv. Space Res. 52, 1146–1154.

Zhang, X., Shen, X., Zhao, S., Yao, Lu., Ouyang, X., Qian, J., 2014. The characteristics of quasistatic electric field perturbations observed by DEMETER satellite before large earthquakes. J. Asian Earth Sci. 79, 42–52.